Normal and Reconstructed Mandibular Condyle Mechanics

S. J. Hollister*
Departments of Biomedical Engineering, Surgery and Mechanical Engineering, The University of Michigan, MI 48109-2125, U.S.A.
S. E. Feinberg
Department of Oral and Maxillofacial Surgery, The University of Michigan, MI 48109, U.S.A.

One approach to reconstructing a damaged mandibular condyle is to replace it with a rib graft. This procedure requires removal of the lateral pterygoid muscle. The rib graft has significantly different shape and mechanical properties than the original condyle. These three factors can be expected to alter mandible (jaw) mechanics. We used voxel-based finite element methods to analysis both normal and a simulated reconstructed mandible using data from the US NIH Visible Human Female. Results demonstrated significant differences between normal and reconstructed mandible mechanics. The reconstructed mandible displaced more than the normal mandible. Stresses in the rib graft were 3 to 4 times higher than in a normal mandibular condyle. Stresses in the rest of the mandible were also higher in the reconstructed case. Further analyses are required to determine how each of the alterations in the reconstructed mandible contributes to the difference in reconstructed mandible mechanics.

Key Words : Mandibular Condyle, CCRG, Voxel Finite Element, Mandibular Mechanics

1. Introduction

There are a number of clinical indications requiring reconstruction of the mandibular condyle, including degenerative joint disease, rheumatoid arthritis, developmental/congenital deformities, trauma and ankylosis. However, mandibular condyle reconstruction remains a significant challenge in Oral/Maxillofacial surgery for which no completely satisfactory answer exists. One of the most efficacious solutions to date for mandibular reconstruction is the grafting of a costhochondral rib to the mandibular ramus following condylectomy, that is, removal of the diseased or damaged mandibular condyle. The costochondral rib graft (CCRG) is used because it provides advantages of an autogenous material, an existing cartilaginous surface, and the possibility of permanent bony union to the existing mandible with a potential for both growth and remodeling. The potential for continued growth and the presence of a cartilaginous cap may be the main reasons the CCRG has enjoyed success to date (Perrot et al, 1994; Raustia et al, 1996). Studies have shown that condylar cartilage, associated with the fibrocartilagenous articular surface, enables the TMJ to withstand compression and loading which assists in the morphological adaptive responses to biomechanical stress (Meikle, 1992). Copray and others (1985) showed mechanical stimuli elicited by joint function can determine the ultimate growth and shape of the condyle.

Despite its advantages the CCRG has four potential drawbacks:

1. The lateral pterygoid muscle is removed during the condylectomy limiting the range of motion

2. The rib shape does not present an exact

* Corresponding Author,
E-mail : scottho@umich.edu
TEL : +1-734-647-9962 ; **FAX** : +1-734-936-1905
Departments of Biomedical Engineering, Surgery and Mechanical Engineering, The University of Michigan, Ann Arbor, MI 48109-2125.

geometric replacement for the temporomandibular joint (TMJ) articulation

3. A second surgical site is required with associated risk of morbidity

4. Growth of the CCRG can be unpredictable in pediatric patients

The first two drawbacks mean that the reconstructed condyle/mandibular tissue mechanics, specifically tissue stress and strain, may differ significantly from normal condyle/mandibular mechanics. Altered tissue mechanics in itself may affect the ultimate long-term outcome of CCRG reconstruction either by directly causing graft failure or by leading to adverse mechanically mediated remodeling of the graft and surrounding tissue. However, the authors know of no specific study addressing how mandibular mechanics are altered due to reconstruction. Such a study is important for two reasons: 1) to determine how much mandibular mechanics are altered following CCRG reconstruction, and 2) if there are significant alterations in mechanics, an analysis may point to potential changes in the surgical procedure to limit mechanical alterations.

2. Methods

Mandibular anatomic data exists primarily in CT or MRI voxel data structures. Although techniques have been developed to mesh complex anatomic structures using traditional finite element meshing techniques, the task remains quite challenging. When significant alterations are made in mandibular anatomy for reconstructive surgery, the entire meshing procedure must be repeated. Due to these difficulties, we chose to directly apply an image-based design and modeling methods to both simulate the reconstructive surgery and to create the finite element models. In this approach, the original image data is first threshold to cortical and trabecular bone to create normal mandible voxel dataset. We used the female CT data of the Visible Human dataset from the US National Library of Medicine. Next, an image-based procedure to simulate the costochondral reconstruction was performed, including condylectomy and rib grafting. This created the costochondral rib graft (CCRG) mandibular reconstruction dataset. Finally, both the normal and CCRG dataset were meshed by directly converting the voxel dataset into voxel-based hexahedral finite elements using the Voxelcon™ software (Quint Corporation, Tokyo, Japan and Voxel Computing Inc, Ann Arbor, MI, USA). The resulting mesh was also analyzed using the Voxelcon software.

The first step in creating the mandibular databases was to segment the original human female CT dataset into cortical and trabecular bone regions. This was done on a slice-by-slice basis using a Region of Interest (ROI) Graphical User Interface (GUI) written in IDL (Interactive Data Language, Research Systems, Inc., Boulder, CO, USA). All cortical bone voxels were set to a density of 4 and all trabecular bone voxels were set to a density of 3. This created the segmented normal mandibular voxel data.

The second step was to simulate the costochondral reconstruction procedure to create the CCRG dataset. First, a simulated condylelectomy was performed by setting all voxels in the trabecular and cortical bone of the mandibular condyle to a density of 0. Next, an outline of a costochondral rib graft was drawn on the mandible with the condylelectomy using the ROI GUI. The costochondral graft was computationally "mortised" into the remaining ramus to mimic the surgical procedure. Finally, a titanium plate to secure the graft to the mandibular ramus was added using the same ROI GUI. In the CCRG dataset, the titanium plate and screw voxels were set to a density of 4, rib graft voxels were set to a density of 3, cortical bone voxels were set to a density of 2, and trabecular bone voxels were set to a density of 1. These steps created the final CCRG voxel data.

The three-dimensional finite element meshes for the normal mandible and the CCRG mandible were created using the Voxelcon software. Using this software, voxel finite elements, 8-node hexahedral elements having the same cubic shape as voxels, are generated to fill the voxel space. The advantage of the voxel-based meshing technique is that any complicated 3D geometry can-

Table 1 Orthotropic properties assumed for the cortical and trabecular bone of the mandible, from Hart et al. (1992)

Bone	E_{xx}(MPa)	E_{yy}(MPa)	E_{zz}(MPa)	G_{xy}(MPa)	G_{yz}(MPa)	G_{xz}(MPa)	n_{xy}	n_{yz}	n_{xz}
Cortical	13000.	13000.	19000.	5300.	5900.	5900.	.22	.29	.42
Trabecular	273.	273.	823.	115.	123.	123.	.19	.34	.11

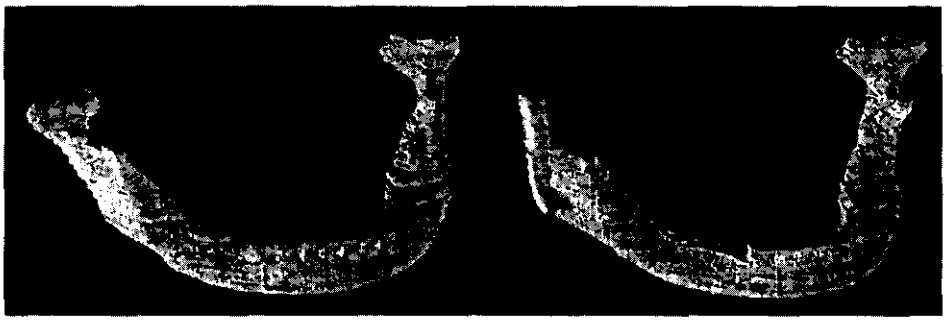

(a) (b)

Fig. 1 Voxel-based meshes for the normal (a) and CCRG (b) mandible. Note that in the CCRG mandible the rib graft with plate is on the right

(a) (b)

Fig. 2 A top view of both the normal (a) and CCRG mandible (b). Note the difference in area and shape of the rib graft (on the right in the CCRG mandible) and the corresponding normal mandibular condyle

not only be automatically meshed, but meshed in minutes. Using the voxel-based meshing method, a model with 236,321 elements was created for the normal mandibular dataset and a model with 208, 519 elements was created for CCRG dataset (Fig. 1).

Note that there is a significant difference in the profile of the normal mandibular condyle and that of the rib graft as seen looking at the top of both the normal and reconstructed mandible (Fig. 2).

The remaining tasks following model generation are input of material properties and boundary conditions. All materials were assumed to be linear elastic. Properties for cortical bone and trabecular bone in both the normal mandible and CCRG model were assumed to be orthotropic as reported by Hart et al. (1992, Table 1). For the CCRG model, rib graft properties were assumed to be isotropic with Young's Modulus E=2700 MPa and n=0.3 based on mechanical tests of seventh thoracic ribs reported by Yoganandan and Pintar (1996). Finally, titanium was modeled as isotropic with E=114,000 MPa and n=0.3.

Four muscle pairs were modeled as force input to the model: left and right anterior temporalis,

Table 2 Assumed force magnitudes for the anterior temporalis, masseter, lateral pterygoid and medial pterygoid muscles (left and right) and joint contact forces (left and right) estimated from Koolstra et al. (1992). Note that in the reconstructed mandible model there is no lateral pterygoid force. Note that the positive X component represents a force directed laterally on the right side and medially on the left side. The positive Y component represents a force in the anterior direction and a positive Z component represents a force in the inferior direction. Thus, the joint contact force is directed inferiorly while the remaining muscle forces act superiorly. All values are given in Newtons

Right Anterior Temporalis	X Component (Medial-Lateral) N	Y Component (Anterior-Posterior) N	Z Component (Inferior-Superior) N
Right Anterior Temporalis	-70	-26	-153
Right Masseter	-20	33	-153
Right Lateral Pterygoid	-27	44	10
Right Medial Pterygoid	37	17	-97
Right Condyle Contact	-50	-345	379
Left Anterior Temporalis	55	-25	-122
Left Masseter	14	22	-169
Left Lateral Pterygoid	-19	56	16
Left Medial Pterygoid	-31	16	-71
Left Condyle Contact	50	345	379

left and right masseter, left and right lateral pterygoid, and left and right medial pterygoid. These are the main muscles active in chewing and exert the greatest force. We chose to model the muscle forces generated during maximum bite force to illustrate the maximum possible stresses generated on the normal and reconstructed mandible. Also, we are interested in tissue engineering approaches to mandible reconstruction and are interested in knowing the maximum stresses that a biomaterial scaffolds must withstand. The muscle forces and associated condyle contact forces were taken from the optimization models developed by Koolstra et al. (1988, 1992; Table 2). The incisors were the only teeth present in the Visible Female dataset. These teeth were fixed with no displacement to simulate a static maximum bite on a hard material. The same force and displacement boundary conditions were applied to both the normal mandibular and CCRG model with the exception that the medial pterygoid muscle force was removed from the reconstructed (right) side. This simulates the actual surgical reconstruction since the muscle is detached during the condylectomy and is not reattached.

The Voxelcon solver was used to analyze the models under the assumed boundary condition. This solver is based on an iterative technique to handle the very large-scale models. An iterative solver satisfies the equilibrium equations to within a tolerance, taken as the residual norm. We used .0001 as the tolerance for convergence. The normal mandible model converged after 8000 iterations while the CCRG model took 16,000 iterations to converge, due to the presence of materials with a much wider range of stiffness that increases the conditioning number of the stiffness matrix. Resulting displacements and stresses were then viewed in the Voxelcon pre/post processor module to compare the difference between the normal mandible and CCRG models.

3. Results

Results show a very complex 3D displacements and stress state in both the normal and CCRG models. Displacement results for the normal mandible model showed bending in the Anterior-

Posterior (AP) [Fig. 3(a)]. CCRG displacement results also showed significant AP bending [Figure 3(b)].

The graft bending was much more pronounced, however, then bending of the corresponding condyle in the normal mandibular model, and the graft displaced more than a corresponding normal condyle. In addition, the contralateral normal condyle of the CCRG displaced more than the same condyle of the normal mandible. This may be due to the fact that the graft was modeled as being much more highly compliant (2600 MPa) than the cortical bone of the condyle (13,000-19,000 MPa) in the current model. These results demonstrate that the displacement field of the CCRG reconstructed mandible differed significantly from that of the normal mandible.

Stress distributions also differed significantly between the normal and CCRG mandible, resulting from different displacement fields. Stresses in the CCRG mandible were in general higher than those of the normal mandible. Graft stresses were

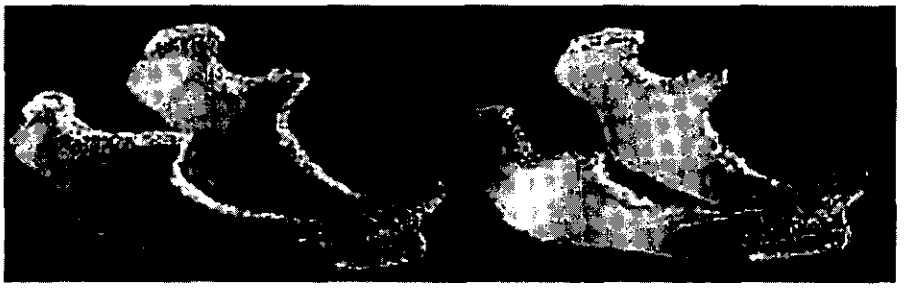

(a) (b)

Fig. 3 Deformation of the normal mandible (a) and CCRG mandible under applied loads. Yellow lines indicate original undeformed shape. Color indicates deformed shape. Blue indicates smaller displacement, while orange and red indicate the highest displacement. Both models show bending in the Anterior-Posterior (AP) plane. Bending displacement is highest for the rib graft (shown in red). The contralateral condyle of the CCRG mandible (shown in green and yellow) also shows increased displacement compared to either condyle in the normal mandible (shown at left in blue)

(a) (b)

Fig. 4 Von Mises effective stresses for the normal mandible (a) and the CCRG mandible (b). The superior border of the mandible experiences high Von Mises stresses in both cases due to the bending deformation. However, stresses in the CCRG mandible are significantly higher than the normal mandible. The condyle experiences very low Von Mises stresses in the normal mandible, in the range of 0 to 4 MPa. The rib graft experiences moderate to high Von Mises stresses (4 to 18 MPa) in the CCRG mandible. Note horizontal scale numbers should be multiplied by 10

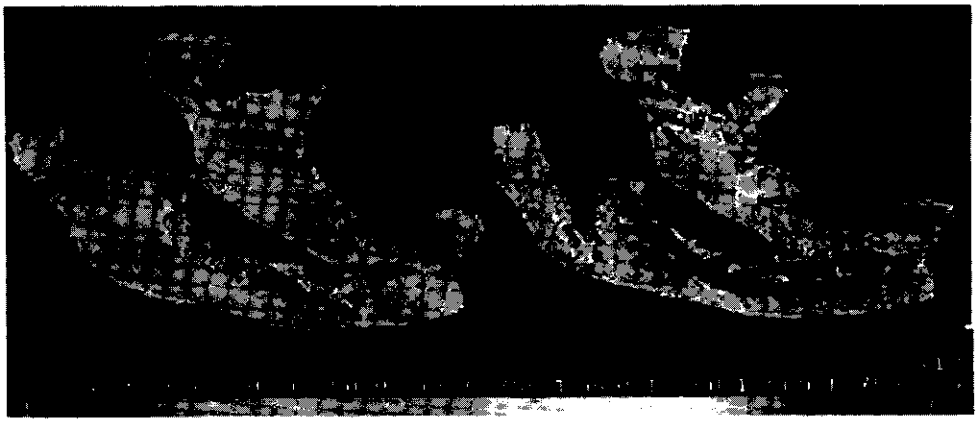

(a) (b)

Fig. 5 Maximum principal stresses for the normal mandible (a) and the CCRG mandible (b). The superior border of the mandible experiences high tensile stresses in both cases due to the bending deformation. However, stresses in the CCRG mandible are significantly higher than the normal mandible. The condyle experiences very low tensile stresses in the normal mandible. The rib graft experiences moderate tensile stresses (up to 8 MPa) in the CCRG mandible. Note horizontal scale numbers should be multiplied by 10

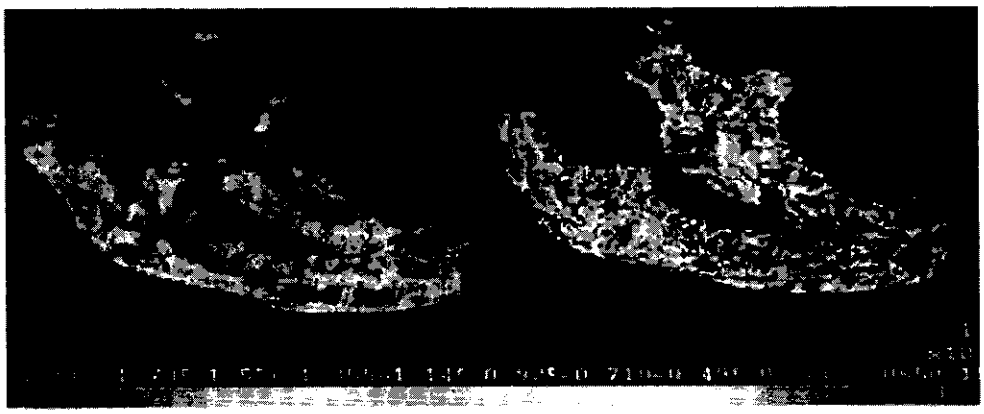

(a) (b)

Fig. 6 Minimum principal stresses for the normal mandible (a) and the CCRG mandible (b). Most of the normal mandible is subjected to compressive stresses less than 3 MPa, as indicated by the red areas. The CCRG mandible experiences significantly higher compressive stresses. The graft itself experiences very high compressive stresses, ranging up to 11 MPa. Note horizontal scale numbers should be multiplied by 10 and blue indicates higher compressive stresses

significantly higher than those of a normal condyle. For example, the rib graft Von Mises stresses reached 12 MPa, while those of the normal mandibular condyle were below 6 MPa. In addition, stresses in the contralateral condyle of the CCRG mandible were higher than that of either condyle in the normal mandible. This was true for Von Mises stress (Fig. 4), maximum principal stresses (Fig. 5) and minimum principal stress (Fig. 6).

4. Discussion

Both stress and displacement results showed significant alterations in the CCRG mandible mechanics as compared to the normal mandible

mechanics. There are three significant difference between the CCRG mandible: 1) the CCRG has no right lateral pterygoid muscle force, 2) the rib graft in the CCRG mandible is much less stiff than a normal condyle (2.6 GPa versus for the rib graft versus a mixture of cortical and trabecular bone in the condyle with stiffness of 13–19 GPa and . 2–.8 GPa, respectively), and 3) the rib graft shape has a smaller area and significantly different shape than a normal condyle (Fig. 3). The difference between normal and CCRG mandible mechanics can be attributed to each of these differences individually or perhaps a combination of two or even three of these differences. The removal of the lateral pterygoid muscle, which acts in the superior and anterior direction, means that there will be less muscle force to counteract the posterior and inferior directed joint contact force. This could contribute to the greater posterior and inferior displacement of the graft. The decreased rib graft stiffness would also lead to increased displacement compared to a normal mandibular condyle under the same load. Finally, the decreased area of the rib graft compared to the normal mandibular condyle would also lead to increased stresses in the graft. Since each of the differences alone would lead to increased displacements and stresses, the combination of these factors would clearly exacerbate the situation causing further increased stresses and displacements in the CCRG mandible versus the normal mandible. Although beyond the scope of the current work, these factors can be readily tested in future studies by 1) increasing the stiffness of the rib graft to assess its impact on CCRG mandible mechanics, 2) reapplying the lateral pterygoid force to the rib graft, and 3) reducing the stiffness of a normal shaped condyle to that of a rib graft to test the affects of condyle replacement shape on mandible mechanics.

As with any modeling study, assumptions must be made for the analysis. There are three assumptions specifically that will influence the results of the current study: 1) assumed muscle forces and boundary conditions, 2) assumed material properties, and 3) assumed mandible and graft geometry. The assumption of boundary conditions and muscle forces will vary significantly between individuals and within an individuals own mastication cycle. Muscle forces in this study were taken from the optimization models of Koolstra and colleagues (Koolstra et al., 1988; Koolstra et al., 1992) for maximum bite force. Koolstra et al. calculated the muscle insertion sites and line of force, (1992) for seven subjects using MRI data and are as representative as any available in the literature. Koolstra et al. initially calculated the muscle force magnitudes (1988) using an optimization model to solve the indeterminate static force equilibrium equations. The assumed objective function was to minimize the maximum force generate by any muscle with a constraint that both force and moment equilibrium equations were satisfied. They assumed a maximum bite force that would be the upper limit of force generation. They later verified (Koolstra et al., 1992) this optimization model with EMG data taken on seven subjects and found good correlation between the optimization model results and the experimental EMG data. Thus, the muscle force inputs for the normal mandible model are believed to be as accurate as available in the literature for the normal mandible model. Similar data experimentally verified did not exist for the CCRG model, so the same muscle forces were applied to the CCRG model in the current study as were applied to the normal mandible model. It is possible that the muscle force generation and activation patterns could change with the removal of the lateral pterygoid muscle. Although the current model does account for the loss of the lateral pterygoid muscle, it does not account for changes in the force generation by the remaining muscles. The joint contact forces are those generated in response to a large bite force. These will represent an upper bound on the contact forces, and therefore the models will give an upper bound on the stresses in the mandible.

Material properties of the mandibular cortical bone, mandibular trabecular bone, and the rib graft were taken from either previous models (Hart et al, 1992) or experimental studies (Pintar and Yogathan, 1996). These material properties obviously represent a particular individual or set

of individuals, and material properties will vary between individuals. Since the properties are assumed to be linear elastic, homogeneous modifications in material properties will cause a proportional increase or decrease in stress. Heterogeneous variations in material properties will cause localized fluctuations in stress and strain. It is expected that the general trends regarding changes in mandibular mechanics between normal and CCRG will still hold despite variations in material properties.

Finally, the current model represents the mandibular geometry of one individual, the Visible Human Female, who did not have molars. Again, this model may best represent a selected population of mandibular geometry. Stresses in the main body of the mandible (Figs. 7-9) are likely elevated due to the absence of molars. Mandibles with molars would be expected to have lower stresses. However, the trends showing alterations in mandibular mechanics between CCRG and normal mandibles would be expected to hold between mandibles with the same geometry. In other words, a CCRG mandible with molars would have elevated stresses compared to a normal mandible with molars. Testing the effects of mandible geometry can be done with models using more patient CT datasets.

In conclusion, the current study has shown that there are significant alterations in both mandible displacements and stresses following CCRG mandibular reconstruction. Specifically, significantly higher stresses are seen in the rib graft versus the normal mandibular condyle. In addition, elevated stresses were also seen in the contralateral, non-operated side. Both mandibles underwent bending in the Anterior-Posterior plane, with the CCRG mandible having larger displacements than the normal mandible. The three major differences between the CCRG and normal mandible including 1) loss of the lateral pterygoid muscle, 2) the decreased stiffness of the rib graft compared to the normal mandible and 3) the shape differences between the rib graft and normal mandibular condyle could contribute the increased stresses in the CCRG mandible. These differences should be systematically tested in future models.

References

Copray, J.C.V.M., Jansen, H.W.B., Duterloo, H.S., 1985, "The Role of Biomechanical Factors in Mandibular Condylar Cartilage Growth and Remodeling in Vitro." in *Developmental Aspects of Temporomandibular Joint Disorders*, eds. Carlson DS, McNamara JA and Ribbens K, Monograph Number 16 Craniofacial Growth Series, Center for Human Growth and Development, The University of Michigan, Ann Arbor, Michigan, pp. 235~269.

Hart, R.T., Hennebel, V.V., Thongpreda, N., Van Buskirk, W.C., and Anderson, RC, 1992, "Modeling the Biomechanics of the Mandible: A Three-Dimensional Finite Element Study," *J. Biomech*, Vol. 25, pp. 261~286.

Koolstra, J.H., van Eijden, T.M., 1992, "Application and Validation of a Three-Dimensional Model of the Human Masticatory System in vivo," *J. Biomech*, Vol. 25, pp. 175~187.

Koolstra, J.H., van Eijden, T.M., Weijs, W.A., Naeije, M, 1988, "A Three-Dimensional Model of the Human Masticatory System Predicting Maximum Possible Bite Forces," *J. Biomech*, Vol. 21, pp. 563~576.

Meikle, M.C., 1992, "Remodeling," in *The Temporomandibular Joint: A Biological Basis for Clinical Practice*, eds. Sarnat BG and Laskin DM, WB Saunders & Co. 4th edition. p. 93.

Perrott, D.H., Umeda, H. and Kaban, L.B., 1994, "Costochondral Graft Reconstruction: Reconstruction of the Ramus/Condyle Unit: Long Term follow-Up," *Int J Oral Maxillofac Surg* Vol. 23, pp. 321~328.

Raustia, A., Pernu, H., Pyhtinen, J., and Oikarinen, K., 1996, "Clinical and Computed Tomographic Findings in Costochondral Grafts Replacing the Mandibular Condyle," *J Oral Maxillofac Surg*, Vol. 54, pp. 1393~1400.

Yoganandan, N. and Pintar, F.A., 1996, "Biomechanics of Human Thoracic Ribs," *J. Biomech. Eng*, Vol. 120, pp. 100~104.